Biochemical Engineering Journal 215 (2025) 109617

Contents lists available at ScienceDirect

Biochemical Engineering Journal

journal homepage: www.elsevier.com/locate/bej

Regular article

Individual process steps optimization of *Cupriavidus necator*-catalyzed production of α-humulene

L. Becker [a], E. Dietz [a], D. Holtmann [a,b,*]

[a] Bioprocess Intensification, Institute of Bioprocess Engineering and Pharmaceutical Technology, Technische Hochschule Mittelhessen, Giessen, Germany
[b] Institute of Process Engineering in Life Sciences, Karlsruhe Institute of Technology, Karlsruhe, Germany

ARTICLE INFO

Keywords:
Process optimization
α-Humulene
Cupriavidus necator
Sesquiterpenes

ABSTRACT

The global demand for the valuable sesquiterpene α-humulene is experiencing a period of sustained growth, with applications covering a diverse range of sectors, including food, fragrances, cosmetics, and pharmaceuticals. Until now, the microbial α-humulene production using *Cupriavidus necator* has been conducted under non-optimized process conditions, despite the enormous advantages this method offers over traditional extraction from plants or a chemical synthesis of α-humulene. In this study, the established process parameters, including the composition of the minimal medium, the L-rhamnose induction and the process temperature, were varied and optimized using shake flasks. Furthermore, the *C. necator*-based α-humulene production process was divided into two temperature stages. When compared to the initial conditions, these optimizations resulted in an enhanced *C. necator* growth and/or elevated α-humulene levels. The combination of all individual optimizations into an integrated process led to a notable increase in sesquiterpene levels, from 9.5 to 32.4 mg/L, representing a 241 % increase compared to the initial conditions without any optimizations.

1. Introduction

The terpenome, which includes terpenes and their subgroups, represents the largest group of natural products, with over 80,000 different structures described [1]. Terpenes exhibit a high degree of structural diversity and are involved in a multitude of essential functions and metabolic processes across a vast array of organisms, spanning from plants to microorganisms and animals. The diversity of terpenes is contingent upon the availability of two precursor molecules: isopentenyl pyrophosphate (IPP) and dimethylallyl pyrophosphate (DMAPP). In eukaryotes, some archaea, and gram-positive prokaryotes, the precursor molecules IPP and DMAPP are formed via the mevalonate pathway (MVA). In contrast, in plants and the majority of prokaryotes, they are formed by the methylerythritol phosphate pathway (MEP) [2]. Sesquiterpenes (C_{15} structure), such as α-humulene, also known as α-caryophyllene, constitute a subgroup of terpenes. The sesquiterpene α-humulene is a valuable natural compound found in a multitude of plants, including its namesake, the hop (*Humulus lupulus*), cannabis (*Cannabis sativa*), sage (*Salvia officinalis*), and even in some marine eukaryotes, such as brown algae (*Padina tetrastromatica)* [3,4]. The broad range of applications in the fragrances, food, and cosmetic industries [5–7], as well as its potential pharmaceutical properties against cancer and inflammatory diseases [8–10], has resulted in an increased demand for its production. The microbial production of α-humulene offers significant advantages over traditional plant extraction and chemical synthesis with regard to numerous economic drawbacks, including low yields, high downstream processing costs, and a reliance on fossil-based processes [11,12]. The benefits of a microbial production of α-humulene include economic considerations, controllability, scalability, and the potential for genetic engineering to improve final product levels. *Cupriavidus necator*, a versatile gram-negative bacterium known for its ability to metabolize a wide range of carbon sources such as fructose and CO_2 either heterotrophically or lithoautotrophically, serves as an ideal host for α-humulene production [13].

Due to the natural ability of *C. necator* to autotrophically produce and store up to 82 % [14] or heterotrophically up to 79 % [15] of its cell weight in the biopolymer polyhydroxybutyrate (PHB) under nutrient limitation, a PHB-deficient *C. necator* PHB-4 strain was used in our investigation. This strain diverts the carbon flux required for PHB formation using acetoacetyl-CoA, and accumulates the key intermediate

* Corresponding author at: Bioprocess Intensification, Institute of Bioprocess Engineering and Pharmaceutical Technology, Technische Hochschule Mittelhessen, Giessen, Germany.
E-mail addresses: lucas.becker@lse.thm.de (L. Becker), emely.dietz@lse.thm.de (E. Dietz), dirk.holtmann@kit.edu (D. Holtmann).

https://doi.org/10.1016/j.bej.2024.109617
Received 23 October 2024; Received in revised form 27 November 2024; Accepted 10 December 2024
Available online 11 December 2024

acetoacetyl-CoA for a MVA-pathway-based formation of the terpene precursors IPP and DMAPP [16]. Furthermore, the carbon flux towards the native MEP pathway and terpene production is increased by the absence of a PHB formation under nutrient limitations [17]. The L-rhamnose-inducible production plasmid pKR-hum, transformed into the PHB-deficient *C. necator* PHB-4 strain, carries a recombinant MVA pathway from *Myxococcus xanthus* [11]. In addition to these MVA pathway genes, which extend the native MEP-pathway-based precursor supply, the plasmid pKR-hum contains farnesyl pyrophosphate synthase (*erg20*), α-humulene synthase (*zssI*), and IPP isomerase (*fni*) to convert the precursors IPP and DMAPP via the intermediate farnesyl pyrophosphate (FPP) to α-humulene [18].

Biotechnological processes can be divided into individual biological steps known as unit processing operations (UPOs). Understanding and controlling these UPOs is a prerequisite for a high-quality and robust manufacturing process [19]. As even small changes in cultivation temperature or media composition can have a major impact on the growth of *C. necator* H16 [20] or on bacterial heterogeneity in general, and thus on the efficiency of product formation, this understanding is very essential. For the first time, we have investigated and varied these parameters as well as the published standard conditions for cultivation and induction [17,18,21] of *C. necator* pKR-hum with the aim of developing a simple process optimization strategy. In the literature, *C. necator* pKR-hum grown in lysogeny broth medium achieved a α-humulene level of 10 mg/L after 42 h of production in a heterotrophic batch cultivation [21]. In contrast, *C. necator* pKR-hum grown in the minimal medium [22] used in this study produced α-humulene levels of up to 9.4 mg/L after 52 h [17]. Individual process parameters can often interact with or reinforce each other in unknown and complex ways, which can lead to high variations in bacterial growth and potential product formation. We focused on different parameters to increase the level of α-humulene, including an optimization of the growth media composition, the adaptation of cultivation, and the L-rhamnose induction conditions. In addition to optimizing individual process steps, multiple optimizations were combined into a single process.

2. Materials and methods

All experimental works, including the results presented in chapter 3 and the supplementary information, were carried out in triplicate.

2.1. Heterotrophic cultivation and biomass monitoring of C. necator pKR-hum

In order to establish a stock culture and to ensure comparable starting conditions, *C. necator* pKR-hum cryo cultures were prepared at the start of the study and stored at −80 °C for subsequent testing. *C. necator* pKR-hum was cultivated in 50 mL of a lysogeny broth (LB) medium (in a 250 mL Erlenmeyer flask), supplemented with 15 µg/mL tetracycline (TC) at 30 °C with 180 rpm (Ecotron, Infors HT; Bottmingen, Switzerland). Subsequently, the culture was centrifuged at 5000 g for 5 min, and sterile glycerol was added for cryopreservation. For this purpose, 750 µL of the culture was mixed with 250 µL of sterile glycerol, resulting in a final concentration of 25 % (v/v) glycerol.

The standard procedure for all experiments was maintained consistently to ensure reliable results. Initially, 3 mL of LB medium, supplemented with 15 µg/mL TC, was inoculated in a 15 mL sterile tube as a preculture from a cryo culture of the stock culture. Cells were then cultivated for 24 h at 30 °C with 180 rpm. The appropriate amount of biomass needed to inoculate the main culture to a starting OD_{600} of 0.10 (equivalent to 0.043 g/L biomass, determined by dry mass analysis; see supplementary information, Figure SI - 1) was transferred to a sterile reaction tube, centrifuged, and the pellet obtained was resuspended in 20 mL of the main culture medium, supplemented with 15 µg/mL of TC. The main culture was also cultivated at 30 °C with 180 rpm (Ecotron, Infors HT; Bottmingen, Switzerland) in 250 mL Erlenmeyer flasks, unless other cultivation temperatures were stated. During the main cultivations, the biomass was monitored online in terms of backscattered light intensity measuring every 60 s using the Cell Growth Quantifier device (CGQ, Scientific Bioprocessing; Pittsburgh, USA). To calibrate and adjust the recorded backscatter values, offline OD_{600} measurements were taken just before the start and immediately after the end of the main cultivation.

2.2. Preparation and composition of preculture and main culture media

The standard composition of the minimal medium (MMasy) used for all cultivations, according to Sydow et al. [22], is shown in Tables 1 and 2. To prepare the minimal medium, stock solutions were prepared with deionized water in the same way as the individual components listed in Table 1. After dissolving the media components, all stock solutions, except the trace element stock (Table 2), were autoclaved and stored at room temperature. This standard composition of the minimal medium was used in all experiments, unless other compositions were specified. LB and super-optimal broth (SOB) preculture media were prepared according to the standard recipes; see the following Tables 3 and 4.

To prepare the trace element stock solution, all components listed in Table 2 were dissolved together in 0.1 M hydrochloric acid at a concentration 20,000 times that of the medium, and then filter-sterilized. The trace element stock solution was then stored at 4 °C until it was added 20,000 times diluted to the minimal medium.

The following Tables 3 and 4 list the standard compositions of the LB and SOB preculture media used in this study.

2.3. Microbial α-humulene production using C. necator pKR-hum

Cupriavidus necator H16 PHB-4 was utilized as the host organism for the production of microbial α-humulene. This PHB-deficient strain was transformed by conjugation with the plasmid pKR-hum [18]. The plasmid pKR-hum contains an L-rhamnose-inducible promoter, in addition to the MVA pathway genes, the genes required for the production of α-humulene (*zssI* and *erg20*). A tetracycline resistance gene is present as a marker. The pKR-hum plasmid map is shown in the supplementary information (Figure SI - 2). For standard process conditions, *C. necator* pKR-hum main cultures were cultivated as described in chapter 2.1 and induced at an optical density OD_{600} between 0.50 and 0.70 (*C. necator* pKR-hum biomass 0.2–0.3 g/L) with a final concentration of 0.2 % (v/v) L-rhamnose to initiate α-humulene production, unless otherwise stated, which was achieved by a hundredfold dilution of a 20 % (w/v) L-rhamnose stock solution prepared in deionized water. The stock solution was filter-sterilized and stored at −20 °C. Extracellular α-humulene was removed from the culture process through *in situ* product removal. To achieve this, 4 mL of n-dodecane was added to 20 mL of cultivation broth as a suitable and biocompatible extraction agent after induction [23], corresponding to 20 % (v/v) pure n-dodecane. This created a second phase above the cultivation broth, from which samples were taken immediately after induction and the addition of n-dodecane, as well as at 8, 24, and 48 h later.

Table 1
Standard composition of the minimal medium used (MMasy), stock solutions corresponding to [1]) 10-fold, [2]) 100-fold, and [3]) 20,000-fold final media concentrations.

Media component	Media concentration [g/L]
Na_2HPO_4[1])	2.895
$NaH_2PO_4 * H_2O$[1])	2.707
K_2SO_4[1])	0.170
$CaSO_4 * 2\ H_2O$[1])	0.097
$MgSO_4 * 7\ H_2O$[2])	0.800
$(NH_4)_2SO_4$[2])	0.943
Trace elements[3])	1:20,000 from stock
D-fructose[2])	4.0

Table 2
Trace element composition of the minimal medium used (MMasy).

Trace element component	Media concentration [µg/L]
$FeSO_4 * 7 H_2O$	750
$MnSO_4 * H_2O$	120
$ZnSO_4 * 7 H_2O$	120
$CuSO_4 * 5 H_2O$	24
$Na_2MoO_4 * 6 H_2O$	90
$NiSO_4 * 6 H_2O$	75
$CoSO_4 * 7 H_2O$	2

Table 3
Composition of the lysogeny broth (LB) preculture medium.

Media component	Concentration [g/L]
Yeast extract	5
Tryptone	10
NaCl	5

Table 4
Composition of the super optimal broth (SOB) preculture medium.

Media component	Concentration [g/L]
Yeast extract	5
Tryptone	20
NaCl	0.5
KCl	0.186
$MgSO_4 * 7 H_2O$	2.4

2.4. Quantification of fructose using high performance liquid chromatography (HPLC)

The fructose content of filter-sterilized cultivation samples was analyzed by HPLC (1260 Infinity II, Agilent Technologies; Santa Clara, USA) using the Aminex HPX-87H column (Agilent Technologies; Santa Clara, USA). The elution was performed using 5 mM H_2SO_4 at a flow rate of 0.6 mL/min, and the column oven temperature was set at 50 °C. A multiple wavelength detector (1260 Infinity II Multiple Wavelength Detector, Agilent Technologies; Santa Clara, USA) was used for the detection of fructose at 191 nm. The calibration curve, including the linearity range, as well as an example chromatogram with retention time for fructose HPLC analysis, are provided in the supplementary information (Figure SI - 3).

2.5. Quantification of α-humulene using gas chromatography (GC-MS)

Due to the low water solubility of the product α-humulene in the fermentation broth, *in situ* product removal was performed. For this purpose, the extracellularly released α-humulene was extracted into a 20 % (v/v) n-dodecane phase (4 mL), which was present in the Erlenmeyer flask during the fermentation process. Since n-dodecane is lipophilic, it forms an upper phase from which samples can be collected and further processed for analysis. 100 µL of the centrifuged (5 min, 1000 g) n-dodecane upper phase was taken and stored at −20 °C in GC glass vials until measurement. Just prior to measurement, the samples were diluted with 900 µL acetone. In addition to the samples, calibration standards were created using an α-humulene stock solution (83351, PhytoLab; Vestenbergsgreuth, Germany). The corresponding volumes of pure α-humulene stock solution were diluted in n-dodecane to a final volume of 100 µL and subsequently mixed with acetone at a ratio of 1:10. Samples and standards were prepared by using the same method. As a top standard for the calibration curve, a concentration of 100 mg/L α-humulene was set. The concentration values presented in this study were converted and related to the aqueous culture phase. The detection of α-humulene was performed by gas chromatography and mass spectrometry GC-MS (7890B GC-MS with 5977B GC/MSD, Agilent Technologies; Santa Clara, USA) with an N_2 gas flow of 45 mL/min, air flow of 450 mL/min, and FID of 250 °C. Samples and standards were analyzed using an HP-5ms GC column (Agilent 19091S-433, Agilent Technologies; Santa Clara, USA) with 100 % acetonitrile as the rinsing solvent. The injection volume for the samples was 1 µL. The analysis was carried out using the single ion monitoring method (SIM) at a m/z ratio of 204.2 for α-humulene. The calibration curve, including the linearity range, as well as an example chromatogram with retention time for α-humulene analysis by GC-MS, are provided in the supplementary information (Figure SI - 4).

3. Results and discussion

3.1. Optimized sugar concentration in minimal media

The growth of *C. necator* pKR-hum at different fructose concentrations between 2 and 32 g/L in standard minimal medium was recorded in an uninduced (Fig. 1 - A) and an induced culture (Fig. 1 - B).

Additionally, the maximum growth rate μ_{max}, the residual fructose content after 24 h, yield coefficients $Y_{X/S}$, $Y_{P/X}$ and $Y_{P/S}$, and α-humulene levels after 16 h of production were determined as growth and production characteristics (Table 5). Please refer to the supplementary information (Formulas 1–4) for details on the calculation of maximum growth rate values and the yield coefficients.

Different starting concentrations of fructose in the minimal medium were reflected in the growth behavior of *C. necator* pKR-hum (Fig. 1 - A and B). Adding n-dodecane to extract the α-humulene in the induced state (Fig. 1 - B) influenced and increased the measured backscatter values. A fructose concentration of 2 g/L resulted in an early stationary phase after 18 h with a final biomass of 0.70 and 0.94 g/L in the uninduced (Fig. 1 - A) and induced state (Fig. 1 - B), respectively. The highest fructose concentration of 32 g/L resulted in a late stationary phase and a prolonged exponential phase in both cases. Fructose concentrations of 4, 8, and 16 g/L in the induced state (Fig. 1 - B) performed similarly to the concentrations of 8 and 16 g/L in the uninduced state (Fig. 1 - A).

In summary, a similar *C. necator* pKR-hum growth behavior was monitored at fructose concentrations ranging from 8 to 32 g/L in both the uninduced and induced states.

Initial fructose concentrations of 8 and 16 g/L in the minimal medium proved to be suitable for a prolonged cultivation and a sufficient α-humulene production, with final biomasses of up to 1.3–1.5 g/L and $Y_{P/X}$ of up to 4.35 ± 0.85 mg α-humulene per g biomass (see Table 5). Lower fructose concentrations, such as 4 g/L, showed no residual fructose content after 24 h process time in the induced state, as the induced formation of the product α-humulene, combined with the plasmid-induced metabolic burden, represents an additional load on the metabolism compared to plasmid-free cells [24]. A fructose concentration of 2 g/L clearly limits growth, with a low final biomass of 0.70 and 0.94 g/L achieved in both the uninduced and induced cultures. Too high levels of fructose in the minimal medium can also negatively affect *C. necator* growth, for example, through osmotic stress or an imbalance in carbon metabolism due to excessive fructose uptake rates. These limitations of cell growth, which were observed at too low (2 g/L) or too high (32 g/L) fructose concentrations, have also been described in the literature, where fructose concentrations between 5 and 25 g/L have proven to be reliable for the cell growth of *C. necator* H16 [20]. In addition to the influence of the fructose concentration on growth and carbon metabolism, secondary factors, such as the availability of inorganic nutrients in the medium described by the C/N/P ratio [25], also exert an effect.

In consideration of the observed growth behavior of *C. necator* pKR-hum and the high yield coefficients, a concentration of 8 g/L fructose was confirmed as suitable in this study. Additionally, residual fructose was observed at the end of the α-humulene production process, indicating that a carbon limitation did not occur over the course of the

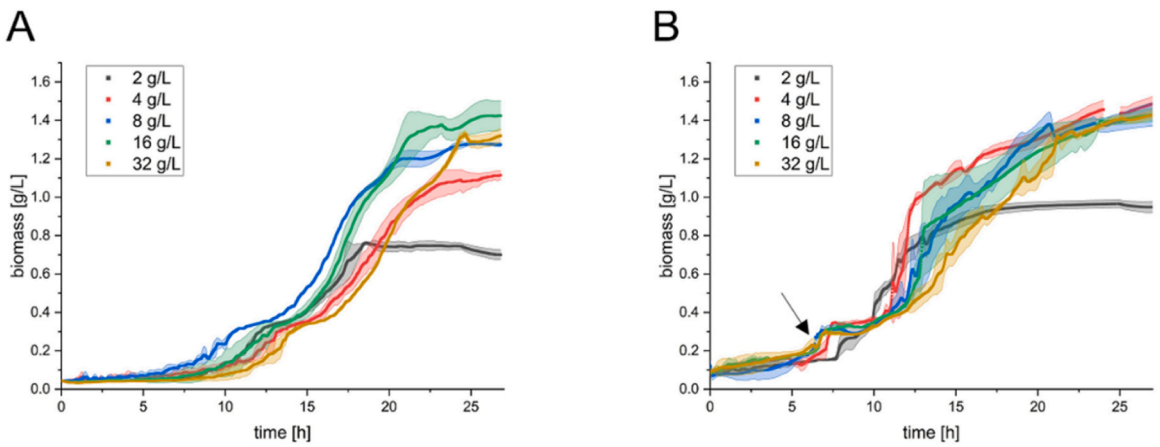

Fig. 1. (A) *C. necator* pKR-hum growth at different fructose concentrations in minimal media, 180 rpm and 30 °C, uninduced; (B) *C. necator* pKR-hum growth at different fructose concentrations in minimal media, 180 rpm and 30 °C, induced with 0.2 % (v/v) L-rhamnose at 0.2–0.3 g/L biomass and the addition of 20 % (v/v) n-dodecane as an extracting agent, see arrow.

Table 5
Performance indicators for the growth of *C. necator* pKR-hum in the uninduced (Fig. 1 - A) and induced (Fig. 1 - B, after 16 h of production) cultures.

$C_{fructose\ initial}$ [g/L]	μ_{max}		$C_{fructose\ 24\ h}$ [g/L]		$Y_{X/S\ 24\ h}$		$Y_{P/X\ 16\ h}$	$Y_{P/S\ 16\ h}$	$C_{\alpha\text{-humulene}\ 16\ h}$ [mg/L]
	no induction	induction	no induction	induction	no induction	induction	induction	induction	induction
2	0.159 ± 0.012	0.230 ± 0.050	0	0	0.351 ± 0.005	0.410 ± 0.033	2.599 ± 0.056	1.067 ± 0.107	2.12 ± 0.12
4	0.147 ± 0.008	0.151 ± 0.013	0.89 ± 0.17	0	0.339 ± 0.041	0.369 ± 0.007	3.201 ± 0.332	1.183 ± 0.140	4.72 ± 0.46
8	0.193 ± 0.012	0.150 ± 0.009	4.91 ± 0.08	4.00 ± 0.60	0.390 ± 0.008	0.349 ± 0.099	3.542 ± 0.469	1.232 ± 0.341	4.57 ± 0.61
16	0.210 ± 0.020	0.155 ± 0.005	12.70 ± 0.30	12.44 ± 0.12	0.405 ± 0.051	0.369 ± 0.029	4.350 ± 0.854	1.623 ± 0.405	5.68 ± 1.16
32	0.177 ± 0.012	0.131 ± 0.009	26.49 ± 0.11	28.26 ± 0.29	0.232 ± 0.013	0.247 ± 0.018	4.578 ± 0.582	1.748 ± 0.094	6.52 ± 0.16

process. The biomass/substrate yield coefficient $Y_{X/S}$ for fructose is also high at this concentration and indicates efficient biomass formation and fructose utilization (see Table 5). With a value of 0.39 in the uninduced state, it is close to the modeled maximum value of 0.53 for fructose in *C. necator* [26], which, however, does not take into account gene expression and other regulatory factors. The biomass curve of the induced cultivation (Fig. 1 - B), which is based on a backscatter signal, shows a sudden increase after the induction point (black arrow). This increase in the backscatter signal, as well as the higher standard deviations, can be explained by the addition of 20 % (v/v) n-dodecane for *in situ* product removal. In general, the addition of second phase- and droplet-forming solvents, such as n-dodecane to the aqueous cultivation system, could have a disturbing effect on backscattering measurements [27]. With regard to residual fructose contents, and in order to avoid possible limitations, an optimization of the fructose content from 4 g/L to 8 g/L in the minimal medium was implemented. It should be noted that in terms of fructose utilization, a concentration of 4 g/L fructose is the best amount.

3.2. Iron supplements in minimal media

The growth of *C. necator* pKR-hum was measured at various iron (II) chloride tetrahydrate and iron (II) sulfate heptahydrate levels between 1 and 15 times of their standard amount (0.75 mg/L $FeSO_4 * 7\ H_2O$ [21]) in standard minimal medium in an uninduced culture (Fig. 2). For this purpose, the standard composition of the minimal medium was supplemented with the appropriate concentrations of iron (II) sulfate heptahydrate and iron (II) chloride tetrahydrate.

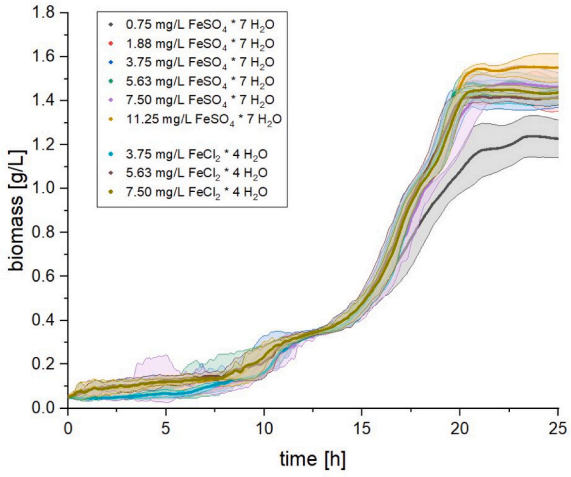

Fig. 2. *C. necator* pKR-hum growth according to different iron (II) sulfate heptahydrate and iron (II) chloride tetrahydrate concentrations in minimal media; 180 rpm and 30 °C, uninduced.

The addition of iron salts to the standard minimal medium containing an iron content of 0.75 mg/L iron (II) sulfate heptahydrate (black line) promotes the growth of *C. necator* pKR-hum (Fig. 2). When the iron salt level is increased 2.5–15 times, the *C. necator* pKR-hum exponential growth phases occur with higher maximum specific

growth rates μ_{max} up to 0.26 ± 0.05 h^{-1} and final biomasses of 1.6 g/L. In comparison to the cultivation with a standard minimal medium containing an iron salt content of 0.75 mg/L iron (II) sulfate heptahydrate without iron supplement, a μ_{max} of 0.17 ± 0.01 h^{-1} and final biomasses of 1.3 g/L were achieved. This effect can be observed from a 2.5-fold increase in the iron salt standard level of the minimal medium, and does not differ between the iron (II) sulfate heptahydrate and iron (II) chloride tetrahydrate salts tested.

Given that iron is an essential nutrient for most organisms and is required for numerous enzymatic processes, as prosthetic groups with a catalytic effect or as cofactors, iron is also involved in a multitude of metabolic processes, cell growth, or cell division [28]. However, no difference in growth behavior could be observed when adding iron (II) sulfate heptahydrate or iron (II) chloride tetrahydrate in the same concentrations. Both compounds optimized the growth behavior equally, depending on their concentrations used, indicating that the iron source has no influence. Consequently, the intracellular iron availability can be increased by an extracellular increase in iron level, as only extracellular iron ions are bound and transported into cells by special proteins like transferrin [29]. Siderophores, such as cupriabactin, have also been shown to promote the growth of *C. necator* JMP134 by increasing the rate of intracellular iron uptake [30]. In addition, the promoted growth observed in this study can also be explained by the protective properties of cupriabactin, as it plays a crucial role in the protection against oxidative stress and toxic aromatic compounds. Many of the protective enzymes involved in these degradation processes require iron in their active enzyme structure and increase their activity through a cupriabactin-induced iron uptake into the cytosol. [30,31]

Gram-negative bacteria, such as *C. necator,* require a minimum iron concentration of 0.017–0.101 mg/L [32] for their growth, which means that the standard iron (II) sulfate heptahydrate concentration of 0.75 mg/L (equals 0.15 mg/L iron) in the minimal medium should adequately cover this requirement. However, we were able to show that a minimal increase in the iron (II) sulfate heptahydrate concentration from 0.75 to 1.88 mg/L is sufficient and results in an increased *C. necator* biomass growth. In order to exclude possible limitations, a 5-fold increase (3.75 mg/L) in the established iron (II) sulfate heptahydrate level was added to the minimal medium for optimization in subsequent experiments.

3.3. Optimization of the L-rhamnose inducer concentration and dosage time

Subsequently, an investigation was conducted to determine the influence of the L-rhamnose inducer concentration and the induction time on α-humulene production. To this end, the α-humulene production of *C. necator* pKR-hum was analyzed after an induction with different concentrations of 0.2, 1, and 2 % (v/v) L-rhamnose at 0.2–0.3 g/L biomass (Fig. 3). Furthermore, the impact of the L-rhamnose induction time on α-humulene production was investigated. Additionally, a potential uptake or consumption of the extracellularly added L-rhamnose over the course of fermentation was evaluated.

We confirmed that *C. necator* pKR-hum does not store or consume L-rhamnose, as the content in the extracellular minimal medium remains constant over the course of fermentation (Figure SI - 5 B). The results also indicate that the final α-humulene production depends on the L-rhamnose induction time; see supplementary information (Figure SI - 6).

The corresponding yield coefficients are shown in the supplementary information (Figure SI - 5 A, C, and D). Fig. 3 illustrates that an elevated L-rhamnose concentration of 2 % (v/v) enhances the final α-humulene level in comparison to the established standard concentration of 0.2 % by 84 and 93 %, respectively, after 24 and 48 h. An increase from 0.2 % to 1 % (v/v) L-rhamnose concentration (green bar) also results in higher product levels.

The pKR-hum plasmid used in this study, for the heterologous expression of α-humulene, is based on a L-rhamnose-inducible system,

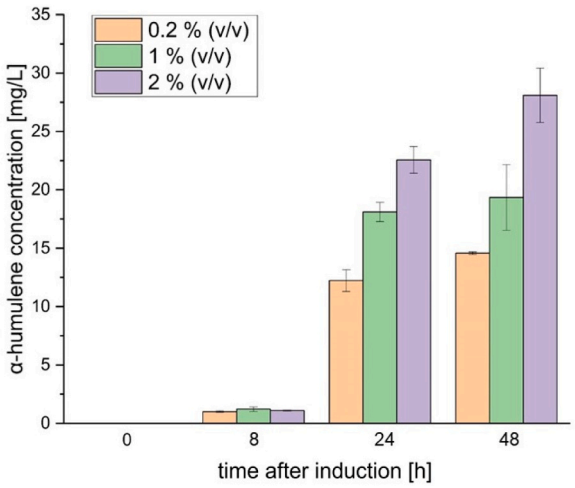

Fig. 3. α-Humulene levels according to different L-rhamnose inducer concentrations in minimal media, at 180 rpm and 30 °C, *C. necator* pKR-hum induced at 0.2–0.3 g/L biomass.

which offers a tight regulation of expression at higher rates compared to other established promoters such as the lactose-inducible P_{Lac} [18]. Varying L-rhamnose levels in *C. necator* pKRrha resulted in a proportional increase in gene expression, as indicated by the increased specific fluorescence of the enhanced green fluorescent protein (eGFP), with 0.18 % (v/v) L-rhamnose (11 mM) yielding the highest gene expression [18]. In later studies, the standard L-rhamnose induction concentration was therefore set at 0.2 % (v/v) [21]. Raising the L-rhamnose concentration from 0.2 % (v/v) to 1 % or 2 % (v/v) resulted in a 33 % or 93 % increase in final α-humulene levels after 48 h. Higher L-rhamnose levels enhance the activation of the transcriptional activator RhaR, triggering rhaSR expression, which leads to RhaS accumulation and the activation of the L-rhamnose operon rhaBAD at the pKR-hum plasmid level, ultimately boosting α-humulene synthase gene expression [33]. The L-rhamnose induction time resulted in lower α-humulene levels after induction at early (0 h) and late (17 h and 21 h) growth phases (Figure SI - 6). Early induction impacts further cell growth and energy metabolism, leading to lower levels. Late induction, close to the stationary phase at reduced cell viability and performance, reduces the final product levels as well. The ideal induction time in the initial exponential phase after 11 h was therefore confirmed for *C. necator* pKR-hum. At this point, the induction time is not too early, which can increase metabolic stress, and not too late, because the growth and performance rates of the culture are high and can be utilized for an increased production [34].

3.4. Batch process with different cultivation temperature stages

In order to investigate a possible influence of the cultivation temperature on α-humulene levels, the formation of α-humulene by *C. necator* pKR-hum as a function of process temperature was investigated (Fig. 4). All cells were incubated at 30 °C with 180 rpm until induction in the range of 0.2–0.3 g/L biomass using 0.2 % (v/v) L-rhamnose. After the induction step, the cultivation temperature was either changed to 25 °C and 20 °C, or kept at 30 °C as the control. These temperatures were maintained until the experiment ended.

The α-humulene level over time, depending on the cultivation temperature, is shown above (Fig. 4). It can be concluded that the highest cultivation temperature of 30 °C leads to the greatest α-humulene levels at the measurement points of 8 and 24 h post-induction. However, reducing the cultivation temperature to 25 °C after induction results in a higher final α-humulene level after 48 h compared to the standard temperature of 30 °C. Specifically, the final α-humulene level increases

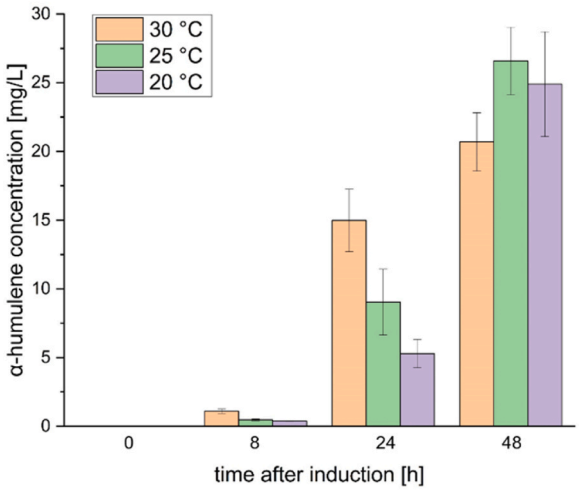

Fig. 4. α-Humulene levels at different cultivation temperatures in minimal media after induction, *C. necator* pKR-hum induced with 0.2 % (v/v) L-rhamnose at 0.2–0.3 g/L biomass, at 180 rpm and 30 °C until induction, then switch to the displayed temperature.

by 28 % at 25 °C and by 20 % at 20 °C compared to the cultivation at 30 °C. The corresponding product yield coefficients $Y_{P/S}$ and $Y_{P/X}$ further support this observation after 48 h, as shown in the supplementary information (Figure SI - 7).

Although lowering the culture temperature from 30 °C to 25 °C slows down the growth behavior of *C. necator* pKR-hum, with a final biomass in a similar range (following chapter 3.5), this reduced cell growth and the subsequent decrease in α-humulene production competes with the benefits of the lower temperature. This explains why, at 8 and 24 h post-induction, the α-humulene level is highest at 30 °C. However, after 48 h, the optimal temperature for production shifts to 25 or 20 °C. Data collected 48 h after induction revealed a significant difference in mean α-humulene levels between 30 and 25 °C, as indicated by an unpaired *t*-test with Welch's correction. The p-value of 0.064, at a significance level of 0.10, suggests that α-humulene levels are higher at 25 than at 30 °C. This indicates that lower temperatures may enhance production efficiency. During this 48 h period, the cells recover from the temperature-related growth slowdown, and the lower temperatures can now exert their positive effect on α-humulene production. For an optimization of the overall process, the temperature was therefore lowered from 30 to 25 °C in the final run no earlier than 24 h after induction.

In *E. coli*, it was shown that the expression of heterologous proteins could be optimized by lowering the cultivation temperature after induction from 37 to 23 °C [35]. Therefore, due to the lower temperatures after induction, it is possible that the enzymes of the MVA pathway α-humulene synthase (*zssI*) and farnesyl pyrophosphate synthase (*erg20*) are formed at a slower translation and folding rate, and that a decrease in protein self-binding and aggregation occurs. This may have led to a higher presence of active proteins in this study. Additionally, research has shown that in *E. coli*, the activity and production of many chaperones increase at lower cultivation temperatures [36]. For example, in *C. necator,* the increased expression and activity of GroESL chaperones contributed to a higher heterotrophic isopropanol production [37]. In other words, these factors combined lead to a better folding and stability of soluble proteins and enzymes at lower temperatures. Since this is a case of heterologous gene expression, and the α-humulene synthase is derived from the ginger plant *Zingiber zerumbet* [17], its optimal temperature may also fall within the lower physiological range, which is generally reported to be between 20 and 40 °C [38]. Given that a temperature of 25 °C is within this range, it may be more favorable for the activity of the α-humulene synthase compared to 30 °C. The increased chaperone activity, improved protein folding, and reduced aggregate formation at lower cultivation temperatures, along with the likely lower temperature optimum of the terpene synthases used, may explain the increased α-humulene production observed in this study at 25 °C as compared to 30 °C.

3.5. Impact of preculture media and cultivation temperature on main culture growth

To investigate the effect of the composition of preculture media on the growth of the main culture, *C. necator* pKR-hum precultures were grown overnight in SOB and LB media. The main cultures were then inoculated to an optical density (OD_{600}) of 0.10 from SOB or LB precultures, and incubated at 30 °C with 180 rpm (Fig. 5 - A). Additionally, the cultivation temperature of the main cultures was varied after inoculating from LB precultures at 25, 30, 32, or 35 °C, and the cell growth was monitored (Fig. 5 - B).

Using a SOB medium as a preculture has a similar effect on the *C. necator* pKR-hum main culture growth behavior compared to a LB medium (Fig. 5 - A), which is why the LB medium was kept as the standard preculture medium. However, the main culture grown in a minimal medium shows a shorter lag phase when inoculated from the SOB preculture compared to the LB preculture. Additionally, the final biomass of the main culture is higher at 1.42 g/L after inoculation from the SOB preculture, compared to 1.30 g/L from the LB preculture. Changing the cultivation temperature from 30 °C to 25 °C also delays the growth of the *C. necator* pKR-hum main culture in the minimal medium, resulting in a longer exponential phase and in a stationary phase that starts up to 6 h later (Fig. 5 - B). The standard temperature of 30 °C promotes the best cell growth among the tested temperatures. When the temperature is increased to 32 or 35 °C, or lowered to 25 °C, the lag- and exponential phases are extended by up to 2.5 h and 6 h, respectively, compared to 30 °C, although the final biomasses remain similar.

The faster growth and the higher final biomass of the *C. necator* pKR-hum main cultures inoculated from SOB medium precultures may be due to the SOB medium being richer in nutrients, containing extra KCl and $MgSO_4$, as compared to the LB medium. This is supported by literature, indicating that magnesium, sulfate, and potassium are important for promoting the growth of *C. necator* [39]. The different cultivation temperatures tested lead to longer lag phases and lower maximum growth rates, this could be observed in *C. necator* when the temperature deviated from the optimal level of 30 °C [40]. The lag phase is prolonged by microbial adaptation processes to lower or higher temperatures, delaying the start of the exponential phase [41]. However, at the end of the cultivation process, the final biomass reached similar levels of 1.30–1.35 g/L across the tested temperature range of 25–35 °C.

3.6. Combined optimization throughout the whole process vs. standard conditions

After optimizing several single steps throughout the production of α-humulene, the key question was how these combined effects would influence the overall process performance. The standard parameters were extended, based on the following insights. Minimal medium optimizations included (i) an increase of fructose from 4 to 8 g/L and (ii) the addition of 3.75 mg/L iron (II) sulfate heptahydrate. For induction step optimizations, (iii) the concentration of L-rhamnose was increased from 0.2 % to 2 % (v/v), and (iv) the cultivation temperature was reduced to 25 and 20 °C, 24 h after the induction step, from an initial temperature of 30 °C. An induction time of 11 h after inoculation (induction step) was set during the initial exponential phase, with biomass ranging from 0.2 to 0.3 g/L, as adopted from standard parameters. α-Humulene levels were measured under both standard and optimized conditions at 25 and 20 °C (Fig. 6).

Fig. 6 illustrates that maintaining a continuous cultivation temperature of 30 °C, along with the established standard parameters (standard run), results in considerably lower α-humulene levels than in the

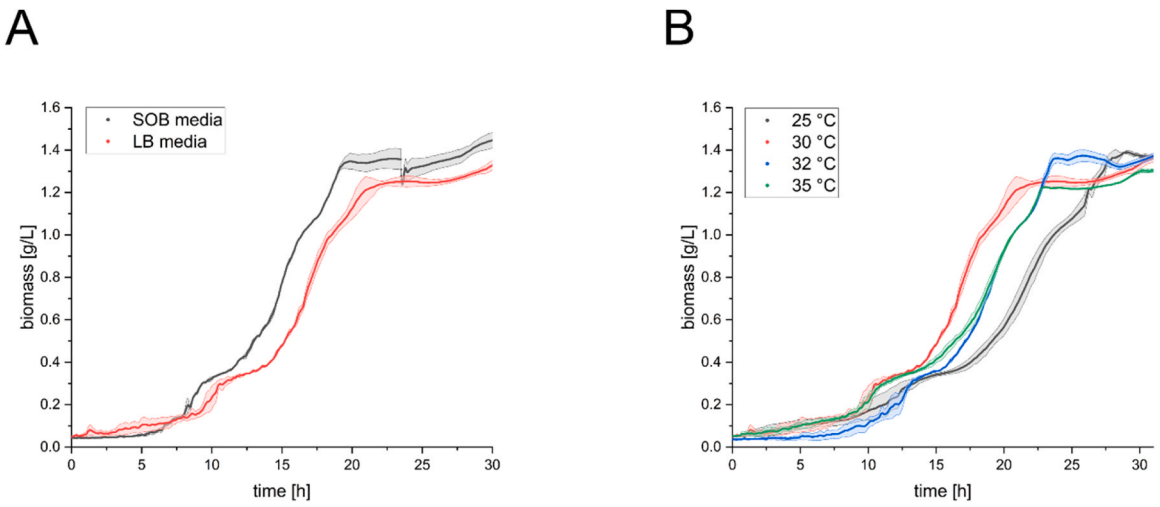

Fig. 5. (A) *C. necator* pKR-hum main culture growth in minimal media following inoculation from lysogeny broth (LB) or super optimal broth (SOB) media precultures, at 180 rpm and 30 °C, uninduced; (B) *C. necator* pKR-hum main culture growth in minimal media at different cultivation temperatures, inoculated from LB precultures, at 180 rpm and uninduced.

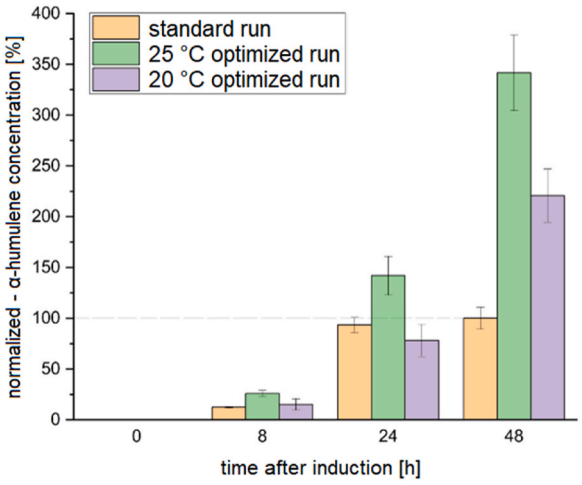

Fig. 6. α-Humulene levels according to standard and optimized conditions and temperatures; *C. necator* pKR-hum, at 180 rpm and 30 °C, standard process induced with 0.2 % (v/v) L-rhamnose at 0.2–0.3 g/L biomass, optimized process induced with 2 % (v/v) L-rhamnose at 0.2–0.3 g/L biomass and switched to 25 and 20 °C cultivation temperature 24 h after induction, α-humulene levels normalized to the 48 h standard run, set as 100 %.

optimized run at 25 °C at the measurement times of 8, 24, and 48 h after induction. Notably, all α-humulene levels were normalized to the 48 h level of the standard run, which was considered as 100 %. With the optimized process conditions, final α-humulene levels increased by 241 % at 25 °C, and by 121 % at 20 °C, after 48 h, compared to the levels achieved under standard conditions at 30 °C after 48 h. These values are normalized for illustration in Fig. 6. The corresponding figure, showing absolute α-humulene levels, can be found in the supplementary information (Figure SI - 8). Corresponding growth measurements indicate that a cultivation with optimized parameters shortens the lag phase, yielding similar final biomass concentrations between 1.50 and 1.55 g/L compared to the established standard conditions. The data are provided in the supplementary information (Figure SI - 9). Increasing the fructose minimal medium content, the iron (II) sulfate heptahydrate minimal medium content, the L-rhamnose induction level, and dividing the batch process into two cultivation temperature stages (30 and 25 °C), led to an optimization of the overall process performance compared to the established standard process parameters.

4. Conclusion

The aim of this work was to optimize the microbial α-humulene production in order to increase the biomass and the terpene production of *C. necator* pKR-hum. The analysis and the variation of the process parameters were successful. The optimized parameters leading to an increased biomass and an increased α-humulene production are a fructose concentration of 8 g/L, an iron (II) sulfate heptahydrate concentration of 3.75 mg/L, a L-rhamnose concentration of 2 % (v/v), and a splitting of the whole process into two cultivation temperature stages of 30 and 25 °C. Combining the optimized individual parameters led to an increased α-humulene level of 241 % compared to the non-optimized process. With this study, we showed that it is possible to optimize the *C. necator*-based α-humulene production process by adjusting the standard parameters. Since the mechanisms and parameter dependencies that led to this additive effect have not yet been investigated, further research and more detailed investigations of the individual effects and the robustness of their impact offer enormous potential.

CRediT authorship contribution statement

Emely Dietz: Investigation. Lucas Becker: Writing – review & editing, Writing – original draft, Visualization, Methodology, Investigation, Data curation. Dirk Holtmann: Writing – review & editing, Supervision, Project administration, Funding acquisition, Conceptualization.

Declaration of Competing Interest

The authors declare that they have no known competing financial interests or personal relationships that could have appeared to influence the work reported in this paper.

Acknowledgments

This research was funded by the Federal Ministry of Education and Research (BMBF), grant number: 01B1050A (project ProNecator). Open Access funding enabled and organized by Projekt DEAL.

Appendix A. Supporting information

Supplementary data associated with this article can be found in the online version at doi:10.1016/j.bej.2024.109617.

Data availability

Data will be made available on request.

References

[1] D.W. Christianson, Structural and chemical biology of terpenoid cyclases, Chem. Rev. 117 (2017) 11570–11648, https://doi.org/10.1021/acs.chemrev.7b00287.

[2] S.T. Withers, J.D. Keasling, Biosynthesis and engineering of isoprenoid small molecules, Appl. Microbiol Biotechnol. 73 (2007) 980–990, https://doi.org/10.1007/s00253-006-0593-1.

[3] J.A. Hartsel, J. Eades, B. Hickory, A. Makriyannis, Chapter 53 - *Cannabis sativa* and Hemp, in: R.C. Gupta (Ed.), Nutraceuticals: Efficacy, safety and toxicity, Academic Press, London, 2016, pp. 735–754, https://doi.org/10.1016/B978-0-12-802147-7.00053-X.

[4] A.A. Behfar, M.R. Shushizadeh, M.H. Far, T.S. Shoar, M. Farasat, E.R. Ghotrami, Gas Chromatography-mass Evaluation of Terpenoids from Persian Gulf *Padina tetrastromatica* sp, AJP (2018), https://doi.org/10.22377/ajp.v12i04.2957.

[5] F. Bakkali, S. Averbeck, D. Averbeck, M. Idaomar, Biological effects of essential oils—a review, Food Chem. Toxicol. 46 (2008) 446–475, https://doi.org/10.1016/j.fct.2007.09.106.

[6] R. Ascrizzi, M. Iannone, G. Cinque, A. Marianelli, L. Pistelli, G. Flamini, Hemping" the drinks: aromatizing alcoholic beverages with a blend of *Cannabis sativa* L. flowers, Food Chem. 325 (2020) 126909, https://doi.org/10.1016/j.foodchem.2020.126909.

[7] H. Jiang, X. Wang, Biosynthesis of monoterpenoid and sesquiterpenoid as natural flavors and fragrances, Biotechnol. Adv. 65 (2023) 108151, https://doi.org/10.1016/j.biotechadv.2023.108151.

[8] L. Becker, D. Holtmann, Anti-inflammatory effects of α-humulene on the release of pro-inflammatory cytokines in lipopolysaccharide-induced THP-1 cells, Cell Biochem Biophys. (2024) 1–9, https://doi.org/10.1007/s12013-024-01235-7.

[9] A.P. Rogerio, E.L. Andrade, D.F.P. Leite, C.P. Figueiredo, J.B. Calixto, Preventive and therapeutic anti-inflammatory properties of the sesquiterpene alpha-humulene in experimental airways allergic inflammation, Br. J. Pharmacol. 158 (2009) 1074–1087, https://doi.org/10.1111/j.1476-5381.2009.00177.x.

[10] Putra I.M.H., Pratama I.P.A.A.C., Putra K.D.A., Pradnyaswari G.A.D., Laksmiani N. P.L. The potency of alpha-humulene as HER-2 inhibitor by molecular docking. 1. 2022; 2:19. doi:10.51511/pr.19.

[11] F. Sonntag, C. Kroner, P. Lubuta, R. Peyraud, A. Horst, M. Buchhaupt, J. Schrader, Engineering *Methylobacterium extorquens* for de novo synthesis of the sesquiterpenoid α-humulene from methanol, Metab. Eng. 32 (2015) 82–94, https://doi.org/10.1016/j.ymben.2015.09.004.

[12] T. Hu, E.J. Corey, Short syntheses of (+/-)-delta-araneosene and humulene utilizing a combination of four-component assembly and palladium-mediated cyclization, Org. Lett. 4 (2002) 2441–2443, https://doi.org/10.1021/ol026205p.

[13] H. Wohlers, L.A. Companioni, D. Holtmann, Chapter 11 *Cupriavidus necator* – a broadly applicable aerobic hydrogen-oxidizing bacterium, Autotroph. Biorefinery (2021) 297–318.

[14] N. Taga, K. Tanaka, A. Ishizaki, Effects of rheological change by addition of carboxymethylcellulose in culture media of an air-lift fermentor on poly-D-3-hydroxybutyric acid productivity in autotrophic culture of hydrogen-oxidizing bacterium, *Alcaligenes eutrophus*, Biotechnol. Bioeng. 53 (1997) 529–533, https://doi.org/10.1002/(SICI)1097-0290(19970305)53:5< 529::AID-BIT11> 3.0.CO;2-B.

[15] S.L. Riedel, S. Jahns, S. Koenig, M.C.E. Bock, C.J. Brigham, J. Bader, U. Stahl, Polyhydroxyalkanoates production with *Ralstonia eutropha* from low quality waste animal fats, J. Biotechnol. 214 (2015) 119–127, https://doi.org/10.1016/j.jbiotec.2015.09.002.

[16] M. Raberg, B. Voigt, M. Hecker, A. Steinbüchel, A closer look on the polyhydroxybutyrate- (PHB-) negative phenotype of *Ralstonia eutropha* PHB-4, PLOS ONE 9 (2014) e95907, https://doi.org/10.1371/journal.pone.0095907.

[17] T. Krieg, A. Sydow, S. Faust, I. Huth, D. Holtmann, CO_2 to terpenes: autotrophic and electroautotrophic α-humulene production with *Cupriavidus necator*, Angew. Chem. Int. Ed. 57 (2018) 1879–1882, https://doi.org/10.1002/anie.201711302.

[18] A. Sydow, A. Pannek, T. Krieg, I. Huth, S.E. Guillouet, D. Holtmann, Expanding the genetic tool box for *Cupriavidus necator* by a stabilized L-rhamnose inducible plasmid system, J. Biotechnol. 263 (2017) 1–10, https://doi.org/10.1016/j.jbiotec.2017.10.002.

[19] L. Becker, J. Sturm, F. Eiden, D. Holtmann, Analyzing and understanding the robustness of bioprocesses, Trends Biotechnol. 41 (2023) 1013–1026, https://doi.org/10.1016/j.tibtech.2023.03.002.

[20] C.C. Azubuike, M.G. Edwards, A.M.R. Gatehouse, T.P. Howard, Applying statistical design of experiments to understanding the effect of growth medium components on *Cupriavidus necator* H16 growth, Appl. Environ. Microbiol (2020), https://doi.org/10.1128/AEM.00705-20.

[21] A. Langsdorf, A.-L. Drommershausen, M. Volkmar, R. Ulber, D. Holtmann, Fermentative α-humulene production from homogenized grass clippings as a growth medium, Molecules 27 (2022) 8684, https://doi.org/10.3390/molecules27248684.

[22] A. Sydow, T. Krieg, R. Ulber, D. Holtmann, Growth medium and electrolyte-How to combine the different requirements on the reaction solution in bioelectrochemical systems using *Cupriavidus necator*, Eng. Life Sci. 17 (2017) 781–791, https://doi.org/10.1002/elsc.201600252.

[23] A. Sydow, L. Becker, E. Lombard, R. Ulber, S.E. Guillouet, D. Holtmann, Autotrophic production of the sesquiterpene α-humulene with *Cupriavidus necator* in a controlled bioreactor, Bioengineering 10 (2023) 1194, https://doi.org/10.3390/bioengineering10101194.

[24] Boy C., Lesage J., Alfenore S., Gorret N., Guillouet S.E. Plasmid expression level heterogeneity monitoring via heterologous eGFP production at the single-cell level in *Cupriavidus necator*. 2020. ⟨https://link.springer.com/article/10.1007/s00253-020-10616-w⟩. Accessed 12 Apr 2024.

[25] M. Amini, H. Yousefi-Massumabad, H. Younesi, H. Abyar, N. Bahramifar, Production of the polyhydroxyalkanoate biopolymer by *Cupriavidus necator* using beer brewery wastewater containing maltose as a primary carbon source, J. Environ. Chem. Eng. 8 (2020) 103588, https://doi.org/10.1016/j.jece.2019.103588.

[26] M. Janasch, N. Crang, J. Asplund-Samuelsson, E. Sporre, M. Bruch, A. Gynnå, et al., Thermodynamic limitations of PHB production from formate and fructose in *Cupriavidus necator*, Metab. Eng. 73 (2022) 256–269, https://doi.org/10.1016/j.ymben.2022.08.005.

[27] C. Goddeeris, F. Cuppo, H. Reynaers, W.G. Bouwman, G. van den Mooter, Light scattering measurements on microemulsions: estimation of droplet sizes, Int. J. Pharm. 312 (2006) 187–195, https://doi.org/10.1016/j.ijpharm.2006.01.037.

[28] U.E. Schaible, S.H.E. Kaufmann, Iron and microbial infection, Nat. Rev. Microbiol 2 (2004) 946–953, https://doi.org/10.1038/nrmicro1046.

[29] J. Kaplan, Mechanisms of cellular iron acquisition: another iron in the fire, Cell 111 (2002) 603–606, https://doi.org/10.1016/S0092-8674(02)01164-9.

[30] C. Li, L. Zhu, D. Pan, S. Li, H. Xiao, Z. Zhang, et al., Siderophore-mediated iron acquisition enhances resistance to oxidative and aromatic compound stress in *Cupriavidus necator* JMP134, Appl. Environ. Microbiol (2019), https://doi.org/10.1128/AEM.01938-18.

[31] A.E. Tindale, M. Mehrotra, D. Ottem, W.J. Page, Dual regulation of catecholate siderophore biosynthesis in *Azotobacter vinelandii* by iron and oxidative stress, Microbiol. (Read.) 146 (Pt 7) (2000) 1617–1626, https://doi.org/10.1099/00221287-146-7-1617.

[32] E.D. Weinberg, Iron and susceptibility to infectious disease, Science 184 (1974) 952–956, https://doi.org/10.1126/science.184.4140.952.

[33] S.M. Egan, R.F. Schleif, A regulatory cascade in the induction of rhaBAD, J. Mol. Biol. 234 (1993) 87–98, https://doi.org/10.1006/jmbi.1993.1565.

[34] V.T. Ribeiro, E.A. Asevedo, L.T.C. de Paiva Vasconcelos, M.A.O. Filho, J.S. de Araújo, G.R. de Macedo, et al., Evaluation of induction conditions for plasmid pQE-30 stability and 503 antigen of *Leishmania i. chagasi* expression in *E. coli* M15, Appl. Microbiol Biotechnol. 103 (2019) 6495–6504, https://doi.org/10.1007/s00253-019-09948-z.

[35] A. Sivashanmugam, V. Murray, C. Cui, Y. Zhang, J. Wang, Q. Li, Practical protocols for production of very high yields of recombinant proteins using *Escherichia coli*, Protein Sci. 18 (2009) 936–948, https://doi.org/10.1002/pro.102.

[36] M. Strocchi, M. Ferrer, K.N. Timmis, P.N. Golyshin, Low temperature-induced systems failure in *Escherichia coli*: insights from rescue by cold-adapted chaperones, PROTEOMICS 6 (2006) 193–206, https://doi.org/10.1002/pmic.200500031.

[37] J. Marc, E. Grousseau, E. Lombard, A.J. Sinskey, N. Gorret, S.E. Guillouet, Over expression of GroESL in *Cupriavidus necator* for heterotrophic and autotrophic isopropanol production, Metab. Eng. 42 (2017) 74–84, https://doi.org/10.1016/j.ymben.2017.05.007.

[38] S. Hartwig, T. Frister, S. Alemdar, Z. Li, T. Scheper, S. Beutel, SUMO-fusion, purification, and characterization of a (+)-zizaene synthase from *Chrysopogon zizanioides*, Biochem. Biophys. Res. Commun. 458 (2015) 883–889, https://doi.org/10.1016/j.bbrc.2015.02.053.

[39] P. Passanha, S.R. Esteves, G. Kedia, R.M. Dinsdale, A.J. Guwy, Increasing polyhydroxyalkanoate (PHA) yields from *Cupriavidus necator* by using filtered digestate liquors, Bioresour. Technol. 147 (2013) 345–352, https://doi.org/10.1016/j.biortech.2013.08.050.

[40] V. Lambauer, R. Kratzer, Lab-scale cultivation of *Cupriavidus necator* on explosive gas mixtures: carbon dioxide fixation into polyhydroxybutyrate, Bioengineering 9 (2022) 204, https://doi.org/10.3390/bioengineering9050204.

[41] L. Nicola, E. Bååth, The effect of temperature and moisture on lag phase length of bacterial growth in soil after substrate addition, Soil Biol. Biochem. 137 (2019) 107563, https://doi.org/10.1016/j.soilbio.2019.107563.